ELSEVIER

Journal of Molecular Catalysis A: Chemical 113 (1996) 379–391

JOURNAL OF MOLECULAR CATALYSIS A: CHEMICAL

Dioxygen chemistry of nickel(II) dioxopentaazamacrocyclic complexes: Substituent and medium effects

Chien-Chung Cheng [1], Julia Gulia, Steven E. Rokita [2], Cynthia J. Burrows [*,3]

Department of Chemistry, State University of New York, Stony Brook, NY 11794, USA

Received 23 February 1996; accepted 2 May 1996

Abstract

Nickel(II) complexes of certain dioxopentaazamacrocycles are known to react with dioxygen, but the reaction is highly ligand dependent, includes an induction period, and appears to require ligand oxidation concomitant with O_2 uptake.

Keywords: Autoxidation; Dioxygen; DNA; Macrocycle; Nickel

1. Introduction

While nickel(II) is well established as a redox active metal ion, the number of nickel(II) complexes capable of interaction with dioxygen are few. Examples include square planar and pentadentate complexes derived from such ligands as tri- and tetrapeptides [1], reduced salens [2] and thioether pendant salens [3], and other tetradentate Schiff base complexes [4,5]. Nickel(II) bis-acetylacetonate-type complexes are known to promote autoxidation of aldehydes [6,7].

Of particular interest in the present study are the nickel(II) complexes of a series of pentaazamacrocycles such as **1**(see Fig. 1) that have been reported by Kimura and coworkers to form stable and reversible O_2 adducts [8] in aqueous or methanolic solutions. While **1** is capable of catalyzing the aerobic oxidation of benzene to phenol [9], nickel complexes of both **1** and **2** mediate O_2-dependent DNA cleavage [10]. Despite these intermolecular oxidations, one of the major products of reaction of this class of compounds with dioxygen is ligand oxidation, particularly hydroxylation at C15 [11]. In order to explore the utility of nickel pentaazamacrocy-

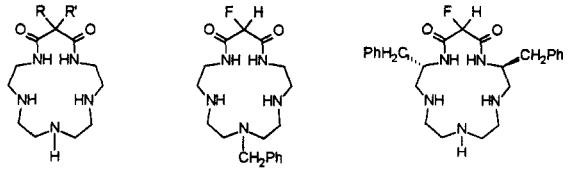

Fig. 1. Dioxopentaazamacrocyclic ligands for nickel(II) complex formation.

* Corresponding author.

[1] Current address: Institute of Chemistry, Academia Sinica, Taipei 11529, Taiwan ROC.

[2] Current address: Department of Chemistry and Biochemistry, University of Maryland, College Park, MD 20742, USA.

[3] Current address: Department of Chemistry, University of Utah, Salt Lake City, UT 84112, USA.

PII S1381-1169(96)00215-4

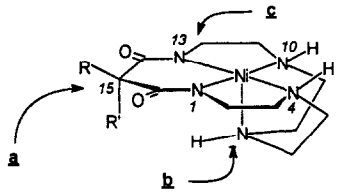

Fig. 2. Possible sites for appendage of DNA-binding substituents, $\underline{a}$ = C15, $\underline{b}$ = N7, $\underline{c}$ = C2, C12.

cles in catalytic oxidation of organic and biological substrates, we have undertaken further mechanistic studies including the synthesis and characterization of additional members of this ligand class.

The ability to append a DNA-binding substituent to a metal chelate reactive with O_2 would be appealing since it could then lead to in vivo applications [12]. Potential positions for introduction of such substituents include the polyamine backbone (such as C2), the amine nitrogens (such as N7), and C15 of the malonate portion of the ligand (Fig. 2). Macrocycles **3** and **4** have already been reported as unreactive with O_2 [10] despite their relatively low $E_{1/2}$ values for the $Ni^{III/II}$ couple. Thus, disubstitution at C15 appears to prevent reaction with dioxygen. Herein we report the synthesis of two new ligands, **5** and **6**, bearing benzyl substituents on the polyamine portion of the ligand, their nickel coordination properties and O_2 reactivity.

2. Results and discussion

2.1. Ligand design and synthesis

An ultimate goal is preparation of O_2-reactive transition metal complexes with DNA-binding substituents such as cations (lysine or arginine derived) or potential intercalants (tryptophan derived). Thus, we sought methods to incorporate amino acids or their sidechain analogs into the macrocycle synthesis. Use of diethyl fluoromalonate rather than diethyl malonate in the macrocyclization reaction with a pentaamine led to much greater yields [10,13]. Thus, one of the desired substituents at C15 is a fluoro group. The observation that C15-disubstituted nickel complexes were unreactive with O_2 suggested that the second substituent

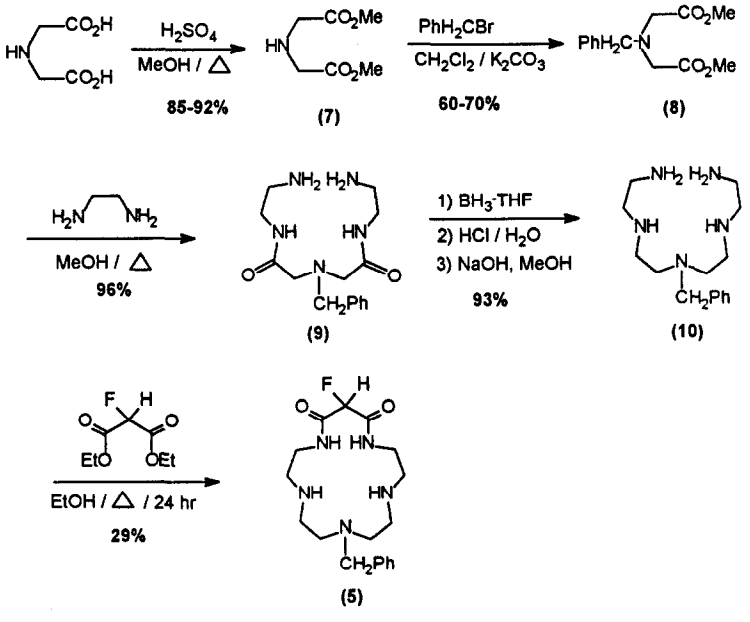

Fig. 3. Synthetic scheme leading to macrocycle **5**.

should be appended at a site other than C15. In terms of ease of synthesis, introduction of substituents would be most readily accomplished through functionalization of a suitably protected diethylenetriamine fragment of the macrocycle. In addition, it was deemed desirable to first develop synthetic routes and study O_2 reactivity with a simple substituent, for example, benzyl. As a result, synthetic pathways were developed to the target macrocycles **5** and **6** bearing a 15-fluoro substituent and benzyl substituents elsewhere, and these are shown in Figs. 3 and 4.

The N7 benzyl substituent required for macrocycle **5** was introduced at an early stage by benzylation of dimethyl iminodiacetate **7** to provide **8**. Chain extension to **9** and borane reduction led to the appropriate pentaamine **10** for macrocyclization. The synthesis of the 2,12-dibenzyl macrocycle **6** proceeded along similar lines, but diamine **11** was chosen as the starting material so that the central nitrogen could remain unreactive as an amide during chain elongation with two equivalents of a suitable derivative of phenylalanine. Phenylalanine was N-protected with a carbobenzyloxy group while the C-terminus was activated for coupling as the N-hydroxysuccinimide ester. Removal of the Cbz protecting groups and borane reduction again led to an appropriate pentaamine for macrocyclization. Although cyclization of **10** with diethyl fluoromalonate was relatively efficient providing a 29% yield of **5** after a 24 h reaction time, the more hindered pentaamine **14** required a 7 day reaction time to produce **6** in 21% yield.

2.2. Nickel complexation

In general, the formation of a pentadentate nickel(II) complex with macrocycles **1–6** occurs

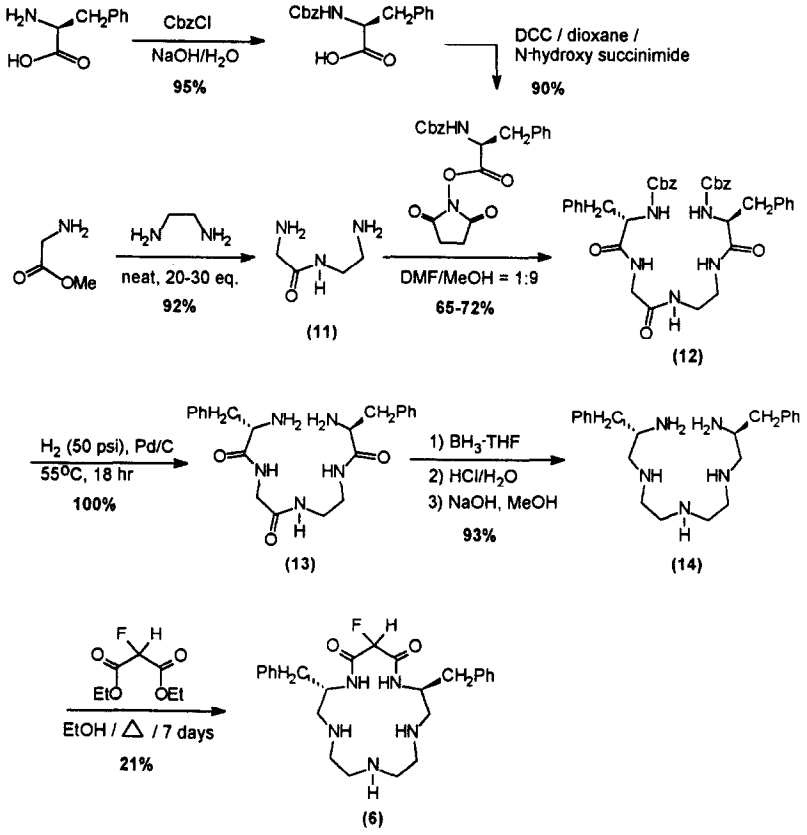

Fig. 4. Synthetic scheme leading to macrocycle **6**.

in a stepwise, base-dependent reaction (Fig. 5). Mixing methanolic solutions of the macrocyclic ligand and $Ni(OAc)_2$ led to initial formation of a green complex (**15** in Fig. 5). For **2 · Ni**, the green complex has been identified as a six-coordinate complex with the three amine nitrogens and one carbonyl oxygen occupying square planar sites and two acetate ions in apical positions [14]. Treatment with two equivalents of base effected amide deprotonation leading to a five-coordinate complex that is purple (**16** in Fig. 5). Double deprotonation is also a stepwise process, the second amide deprotonation being slower than the first [11]. For the parent macrocyclic ligand (R = R′ = H), a crystal structure has been obtained of the purple complex, indicating square pyramidal geometry with the nickel ion lying 0.224 Å out of the plane formed by two amide and two amine nitrogens [15].

The complexation of ligand **5** with $Ni(OAc)_2$ displayed somewhat different behavior than the others. In this case, the pentacoordinate complex was directly formed upon addition of Ni^{2+} to **5** without the need for base treatment. The infrared spectrum in methanol confirmed that the amide nitrogens are deprotonated; the carbonyl stretch was observed at 1616 cm^{-1} in the complex compared to 1687 cm^{-1} for the free ligand. The **5 · Ni** complex is purple in water, blue in methanol and green in CH_2Cl_2.

Ligand **6** when allowed to complex with $Ni(OAc)_2$ in methanol without base treatment showed features expected for coordination to the three amine nitrogens. The amide carbonyl absorption in the infrared spectrum was observed at 1700 cm^{-1} compared to 1668 and 1678 cm^{-1} for the free ligand. After treating with base, a purple solution was formed with electronic absorbances at 358 and 508 nm. A solid precipitated that proved to be insoluble in most solvents. The infrared spectrum (carbonyl absorption at 1600 cm^{-1}) was consistent with the assignment of deprotonated amides in a five-coordinate complex.

2.3. Dioxygen reactivity

The new macrocyclic complexes **5 · Ni** and **6 · Ni** behave similarly to the previously reported complexes **1 · Ni** and **2 · Ni** in their O_2 reactivity. Specifically, when the purple aqueous solution of **5 · Ni** was exposed to air for 12–15 h, a slow color change to an orange solution with electronic absorbances at 310 nm ($\epsilon = 1040$ cm^{-1} M^{-1}) and 486 nm ($\epsilon = 56$ cm^{-1} M^{-1}) was observed. The control solution

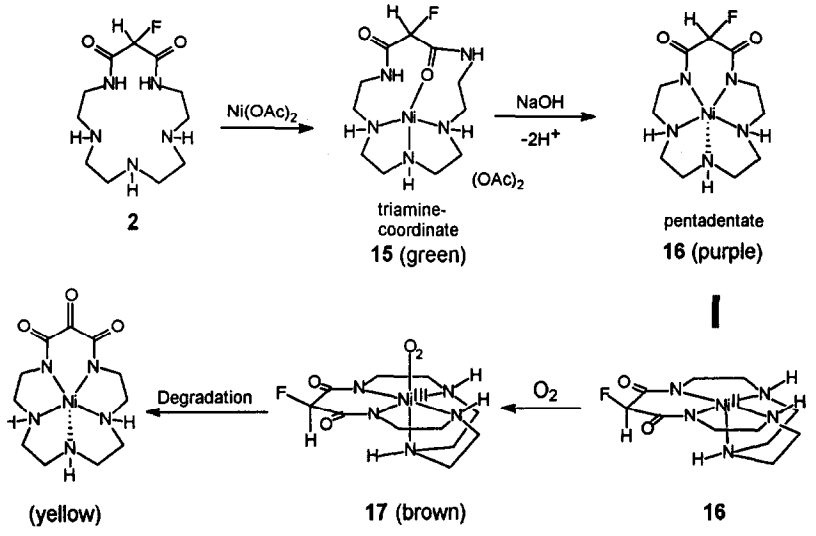

Fig. 5. Proposed mechanism of nickel coordination, O_2 reaction, and ligand oxidation for ligand **2**. Adapted in part from [10].

kept under anaerobic conditions remained purple. Essentially the same results as the aerobic oxidation were obtained if dioxygen was bubbled through the solution. Overall, this behavior is similar to that reported for the nickel(II) complexes of **1** and **2**, but the rate of O_2 reaction is considerably slower when N7 of the macrocycle is substituted with a benzyl group.

Complex **6 · Ni** also appears to react with dioxygen, but the reaction is much more difficult to characterize given the insolubility of the complex. When a suspension of crystals in methanol (or water) were exposed to air for 24–48 h, the colorless solvent gradually turned brown with a UV absorption (of the filtrate) at 310 nm ($\epsilon = 1073$ cm^{-1} M^{-1}) during which time the purple crystals slowly dissolved. After an additional 24–48 h, the color of the solution changed to yellow and all of the crystals had completely dissolved. Thus, substitution of the macrocyclic ligand at C2 and C12 allows the nickel(II) complex to retain O_2 reactivity. However, in the particular case of the dibenzyl-substituted ligand, the insolubility of the complex prevented a detailed study. The oxygenated orange–brown complex is apparently much more soluble, perhaps because it provides additional hydrogen bonding sites to water or methanol solvent molecules. Nevertheless, the results suggest that this is a viable synthetic route allowing incorporation of two sidechains derived from amino acids onto the macrocyclic framework. Other analogs may provide greater solubility and the desired DNA binding ability.

Kimura and coworkers have proposed that the brown complex formed upon exposure of the purple nickel(II) complexes to air is a nickel(III) superoxide complex, shown as **17** in Fig. 5 using ligand **2** as an example. Evidence for this type of structure includes potentiometric measurements of 1:1 adduct formation, UV spectroscopy, electrochemical studies [8] and a preliminary report of ESR measurements [9]. Although the potentials of the purple, pentacoordinate nickel(II) complexes are rather high for O_2 reaction (Table 1), the strength of the nickel–oxygen bond could be a driving force for formation of a Ni^{III}–$O_2^{\cdot-}$ species. Interestingly, the brown intermediate is relatively long-lived, from minutes to nearly an hour depending upon the reaction conditions and the structure of the ligand. Despite support for structure **17**, the accumulated evidence points to a role for a hydrogen atom at C15 in the process of oxygen uptake. Not all pentaazamacrocycles bearing a C15-hydrogen are capable of O_2 reaction, but in no case in this class of ligands have we or others seen O_2 reactivity without a C15 hydrogen. Thus, the hydrogen substituent, or the ability to oxidize C15, appears to be a necessary but insufficient criterion for O_2 reaction. Kimura and coworkers have also shown through a thorough study of changes in the macrocyclic framework (ring size, donor type, and spacial arrangement of donors) that the malonate unit is essential for O_2 reaction [8]. Placing the amide nitrogens in other positions in the macrocyclic deletes reactivity with dioxygen.

These observations, taken together with the work of Chen et al. on hydroxylation of the ligands like **1** [11], suggest ligand autoxidation as a requirement for nickel(II)–O_2 reaction. To lend further support to this hypothesis, we attempted to determine the products of ligand oxidation with some of the new ligands. For compound **2**, the dioxygen reaction ultimately

Table 1
Dioxygen reactivity of nickel(II) complexes of dioxopentaazamacrocycles

R, R' [a]	$E_{1/2}$ (V versus SCE)	O_2 reactive?	Ref.
H, H	0.24	yes	[8]
H, Et	0.24	yes	[8]
H, Bn (**1 · Ni**)	0.24	yes	[8]
H, F (**2 · Ni**)	0.32	yes	[10]
F, F (**3 · Ni**)	0.42	no	[14]
F, Bn (**4 · Ni**)	0.34	no	[10]
H, F (**5 · Ni**)	0.36	yes	this work
H, F (**6 · Ni**)	n.d. [b]	yes	this work
Me, Me	0.17	no	[16], this work

[a] Substituents at the C15 position. Complex numbers given in parentheses refer to Fig. 1.
[b] Not determined due to insolubility.

leads to formation of a yellow nickel(II) complex after decomposition of the brown species. Mass spectral analysis suggests that hydroxylation at C15 may have occurred, but that this is followed by loss of HF from the resulting fluorohydrin to produce a tricarbonyl compound (Fig. 5). A molecular ion (M + 1) in the FAB-MS spectrum at $m/z = 329$ is consistent with this interpretation. In addition, ^{19}F-NMR studies indicated that more than one product is formed. Oxygenation of the N-benzylated complex **5 · Ni** led also to a similar observation in the mass spectrum. In this case, we propose that ligand oxidation leads to debenzylation, perhaps in addition to oxidation at C15. The insolubility of complex **6 · Ni** prevented further characterization of its O_2 reaction and products.

2.4. Factors influencing the rate of O_2 uptake

Because of its ease of synthesis and convenient reaction rate with O_2, complex **2 · Ni** has been the subject of further mechanistic studies as well as applications to DNA cleavage chemistry [10]. Contrary to literature reports [8,11], complexes such as **1 · Ni** and **2 · Ni** show a substantial induction period in their reaction with dioxygen. The dioxygen reaction can be monitored by an oxygen electrode, in which case a decrease in the response of the electrode is observed from an initial point representing air-saturated water that is 240 μM in O_2 (borate buffer, pH 8.1). Data in Fig. 6 compare the decrease in $[O_2]$, presumably due to O_2 uptake by the complex, and the formation of the brown species as monitored concurrently with O_2 uptake at 312 nm in the UV spectrum for compound **2 · Ni**. The nickel(II) complex had been pre-equilibrated in buffer solution to insure complete formation of the purple, pentacoordinate species **16**. An induction period of about 12 min was observed before rapid reaction occurred. After that point, the rate of O_2 uptake and formation of the brown species appear to be equal.

The stoichiometry of O_2 uptake by the fluorinated complex **2 · Ni** was never observed to be 1:1 as reported for the nickel complex of an analog of **1** in which R = R′ = H [8], but rather was approximately 30% of the nickel complex concentration. However, if oxidation at C15 is concomitant with O_2 uptake, it should be pointed out that the difference could be due to the

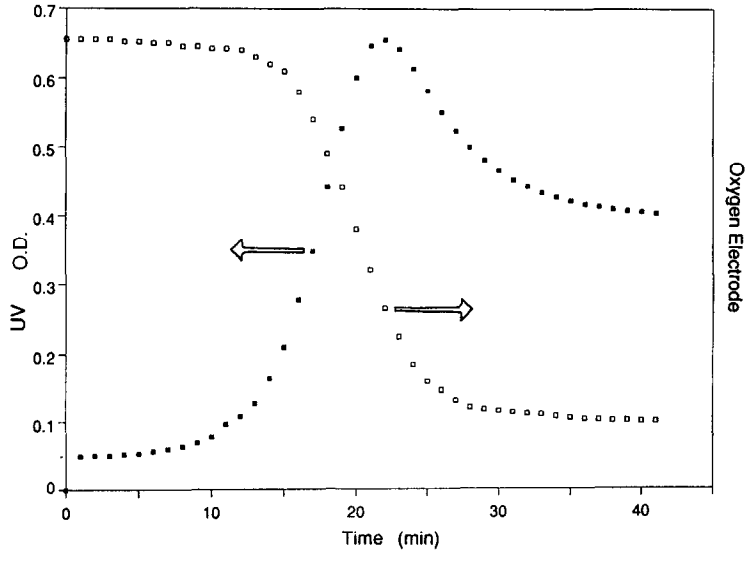

Fig. 6. Optical density at 312 nm (■) and consumption of O_2 as determined by an oxygen electrode (□) measured simultaneously as a function of time for purple complex **2 · Ni** (220 μM) in borate buffer (50 mM, pH 8.1, 25°C).

number of oxidizable hydrogens at C15, two versus one in the present study.

Also evident in Fig. 6 is an eventual decrease in the absorbance at 312 nm. This we attribute to a slow decomposition process leading to oxidized ligand complexes with lower extinction coefficients at that wavelength. The final solution produced in all reactions is yellow in color.

In order to gain further information about the induction period observed for aerobic oxidation of **2 · Ni**, the influence of pH and additional oxidants was studied. When the pH of an aqueous buffered solution was increased in the range 7.6–9.0, a decrease in the induction period was observed. At the same time, the rate of decomposition of the brown O_2-adduct was increased at higher pH to the extent that the intermediate was not observed above pH 8.6, and only the final UV spectrum corresponding to oxidized ligand complex was obtained.

Addition of one-electron oxidants to the system also diminished the induction period, but in this case had little effect on the rate of decomposition of the oxygenated intermediate. For example, substoichiometric amounts of Na_2IrCl_6 ($E_{1/2}$ for $Ir^{IV/III} \cong 0.6$ V versus SCE) in the range of 5–10 mol% compared to **2 · Ni**, dramatically reduced the induction period. The effect was qualitatively but not quantitatively reproducible as shown in Fig. 7. Essentially the same result was obtained by anaerobic electrochemical generation of a nickel(III) complex from the **2 · Ni** purple species and addition to a separate, aerobic solution of **2 · Ni**. Thus, the dioxygenation of **2 · Ni** is autocatalytic in nickel(III).

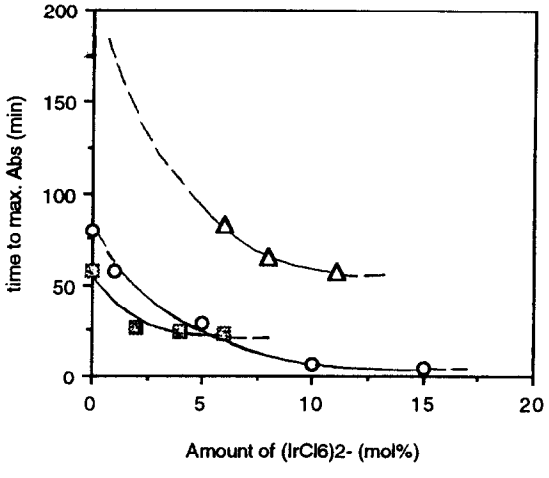

Fig. 7. Three qualitatively reproducible experiments showing the effect of added Na_2IrCl_6 on the induction period for O_2 uptake by purple **2·Ni** (160 μM) as measured by the time required to produce the maximum absorbance at 320 nm associated with the brown O_2 adduct.

3. Conclusions

Accumulating evidence points to the involvement of ligand oxidation as an integral part of the O_2 reactivity of nickel(II) dioxopentaazamacrocycles of the type **1–6**. It appears to be a co-requisite for reaction rather than simply an outcome in the absence of other oxidizable substrates. Clearly intermolecular oxidation can also occur; benzene oxidation and DNA oxidative strand breaks have been observed, although there has been no confirmation of turnover catalysis in this system. Attempts to direct the reactive intermediate formed upon O_2 uptake toward intermolecular chemistry rather than intramolecular ligand oxidation through blockage of the redox active C15 position have not only failed to redirect the oxidation reaction, they have completely shut down the dioxygen pathway. While a component of this failure might be the somewhat higher nickel(III/II) reduction potentials observed with 15-fluoro derivatives, this cannot account for the fact that the 15,15-dimethyl analog (Table 1) whose reduction potential is the lowest in this series (0.17 V versus SCE) did not react with dioxygen. Furthermore, none of the 15,15-disubstituted complexes tested were O_2 reactive even in the presence of $IrCl_6^{2-}$, a species that acted as an initiator in most other cases. Thus, the intriguing question remains:

What is the structure of the brown intermediate formed upon dioxygen reaction with certain nickel(II) complexes?

Many experimental observations must be taken into account in order to propose a mechanism of dioxygen activation in this system. (1) Dioxygen binding has been reported to be 1:1 and reversible for the parent nickel(II) complex (R = R′ = H) [8], but < 1:1 and irreversible for **2 · Ni**. (2) The optimum pH for formation of the brown species is about 8.6. (3) Formation of Ni^{III}, either by chemical or electrochemical oxidation, catalyzes the dioxygen reaction. (4) A redox active malonate unit bearing a C15 hydrogen appears to be required. The nickel(III) superoxide structure **17** is consistent with some, but not all of the data. Specifically, it does not explain the role of the C15 hydrogen. It is not yet known if the non-hydrogen substituents at C15 play a role in anion or radical stabilization, but either type of reactive intermediate might account for some of the observations including the pH dependency and the catalysis by one-electron oxidants. The nickel ion certainly plays a role in the dioxygen reaction, but its binding to dioxygen (Fig. 8, path a) has not been conclusively proven. On the other end of the spectrum, one could propose intermediate **20**, a peroxymalonyl radical whose formation is assisted by electron transfer from a carbanion to a

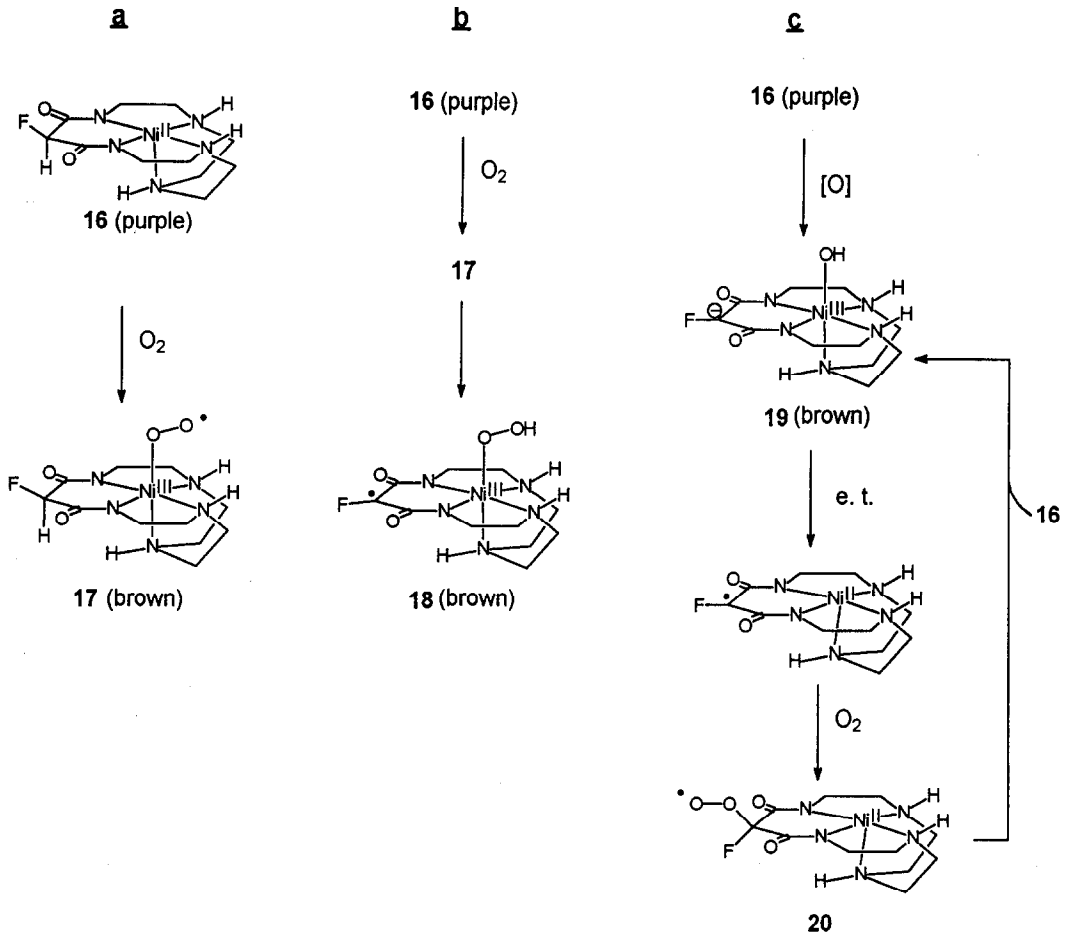

Fig. 8. Mechanistic proposals for 3 alternative pathways of O_2 uptake by **2 · Ni**.

nickel(III) center followed by O_2 quenching (Fig. 8, path c). This pathway would include transient formation of a nickel(III) species, **19**, requiring an induction period. This species is likely the brown complex that accumulates, but it then slowly decomposes by irreversible ligand oxidation at C15. Mechanism c does not include oxygen uptake to produce the first brown species initially; however, O_2 is required to complete the cycle in this autocatalytic mechanism and to generate the next molecule of **19** by reaction with **16**. A compromise mechanism (Fig. 8, path b) would invoke rapid hydrogen atom abstraction from C15 by the nickel(III) superoxide intermediate (**17**) to form a delocalized malonyl radical, **18**. Carbon to nickel(III) electron transfer and carbocation quenching by water would lead to the observed hydroxylated product and release H_2O_2. While pathway b is an attractive alternative, the stability of radical **18** may not be high enough to explain the observation of a relatively long-lived brown intermediate [17].

While the identity of the nickel–dioxygen brown complex awaits further spectroscopic characterization, it is interesting to note the advantages and pitfalls of nickel catalysts for O_2 activation. To date, there are no well characterized examples of nickel–dioxygen complexes that do not also involve ligand oxidation as an apparent co-requisite for reaction. Nickel is a tempting target for dioxygen activation since its redox chemistry is highly dependent upon the ligand architecture, and therefore highly subject to chemists' control. Furthermore, nickel is known to undergo redox processes in vivo leading to oxidative DNA strand breaks and DNA-protein crosslinks in the chemical mechanism of nickel carcinogenesis [18]. Thus, the oxidative chemistry of nickel with amide/amine ligands provides a foundation for understanding biological processes. The oxidations studied here utilize O_2 in an aqueous environment, conditions that are both biomimetic and industrially attractive for catalytic oxidation. The ligand modifications discussed herein have provided insight into the role of a redox active site on the ligand while demonstrating that substituents elsewhere that alter solubility, chirality and potentially DNA targetability, may be tolerated in the oxidation reaction.

4. Experimental

4.1. Materials and instrumentation

Chemicals purchased from Aldrich Chemical and solvents (HPLC grade) from Fisher Scientific were used without further purification unless otherwise noted. ^1H and ^{13}C NMR spectra were obtained on a General Electric QE-300 spectrometer at 300 and 75 MHz, respectively. Infrared spectra were recorded using a Perkin-Elmer 1600 Series FT spectrophotometer. High resolution and FAB mass spectra were obtained on a Kratos MS80RFA spectrometer using a nitrobenzyl alcohol matrix for FAB. UV-visible spectra were recorded on a Hewlett-Packard 8452 diode array spectrophotometer equipped with a HP 89075C programmable multicell transport system. Elemental analyses were performed by Atlantic Microlabs. Electrochemical measurements were carried out on a Bioanalytical Systems 100B electrochemical analyzer. Cyclic voltammograms were obtained in aqueous solutions containing 0.1 M Na_2HPO_4 buffer at pH 9.2 using a glassy carbon working electrode, a platinum auxiliary electrode, and a Ag/AgCl reference electrode. Oxygen consumption was measured on a YSI model 53 oxygen monitor equipped with a YSI 5331 oxygen probe. Oxygen concentrations were determined by a literature procedure [19].

4.2. Ligand syntheses

4.2.1. Dimethyl iminodiacetate (7)

Iminodiacetic acid (29 g, 0.218 mol) was heated to reflux in methanol (300 mL) with conc. H_2SO_4 (40 mL) for 12 h. The solution

was concentrated, water (50 mL) was added, and the solution was rendered basic with solid Na_2CO_3. The aqueous solution was extracted twice with ethyl acetate. The combined organic layers were successively washed with water and brine, dried with $MgSO_4$, and the solvent evaporated, giving 29 g (80%) of a colorless liquid **7**. ^{1}H NMR ($CDCl_3$): 1.97 (s, 1H, –NH), 3.35 (s, 4H, $-N-CH_2-$), 3.61 (s, 6H, $-OCH_3$); ^{13}C NMR: 172.2, 51.7, 49.8.

4.2.2. N-benzyldimethyl iminodiacetate (8)

Benzyl bromide (5.88 g, 0.0345 mol) was added at room temperature to a CH_2Cl_2 (50 mL) solution of diester **7** (6.16 g, 0.0383 mol) and an excess of K_2CO_3 (6.9 g). The solution was heated to reflux for 18 h, then filtered to remove the excess K_2CO_3. Then, 5% aqueous HCl (100 mL) was added, and the solution was extracted twice with CH_2Cl_2. The combined organic layers were washed with water and brine, dried with $MgSO_4$, and the solvent evaporated. The residue was distilled (82–85°C/3 mm Hg) under reduced pressure to remove the unreacted benzyl bromide, leaving 6.8 g (66%) of a yellow liquid **8**. ^{1}H NMR ($CDCl_3$): 7.2–7.5 (m, 5H, –Ph), 3.90 (s, 2H, $-CH_2Ph$), 3.68 (s, 6H, $-OCH_3$), 3.55 (s, 4H, $-NCH_2-$). ^{13}C NMR: 171.6, 138.1, 129.1, 128.5, 127.5, 58.0, 54.1, 51.5.

4.2.3. 7-Benzyl-1,4,7,10,13-pentaazatridecan-5,9-dione (9)

N-Benzyl diester **8** (5.47 g, 0.0218 mol) and ethylenediamine (18 g, 0.30 mol) were heated to reflux in methanol (20 mL) for 18 h. The solvent was removed, and the residue kept under vacuum for 24 h to provide 6.69 g (97%) of a sticky oil, **9**. ^{1}H NMR: 7.80 (t, 1H, –CONH–), 7.1–7.4 (m, 5H, –Ph), 3.65 (s, 2H, $-CH_2Ph$), 3.23 (dd, 4H, $CONH_2-$), 3.15 (s, 4H, $-COCH_2N-$), 2.73 (dd, 4H, $-CH_2NH_2$), 1.84 (s, 4H, $-NH_2$); ^{13}C NMR: 171.0, 137.2, 129.1, 128.4, 127.6, 59.6, 58.4, 44.1, 41.8.

4.2.4. 7-Benzyl-1,4,7,10,13-pentaazatridecane (10)

The diamide **9** (5 g, 0.0163 mol) was heated to reflux in 1.0 M borane–THF (200 mL, 0.20 mol) for 48 h. Excess borane was quenched carefully with methanol (50 mL), and then the solvent was evaporated to leave a residue. The residue was heated to reflux with 6 M HCl (100 mL) for 36–48 h. The solvent was evaporated leaving a white solid. Methanol (50 mL) was added, and the mixture was allowed to cool at 0°C for 6 h. The solid was isolated by filtration and washed with cold methanol to afford a white solid **10** · HCl. ^{1}H NMR (D_2O): 7.49 (m, 5H, Ph), 4.48 (s, 2H, $-CH_2Ph$), 3.2–3.6 (m, 16H, $-CH_2NH-$); ^{13}C NMR (D_2O): 131.2, 130.9, 129.8, 59.3, 48.6, 44.8, 42.2.

In order to obtain the free base, the pentaamine hydrochloride was redissolved in water (20 mL), rendered basic with an excess of NaOH and allowed to stir for an additional 30 min. The solvent was evaporated to leave a mixture containing an oil and a white solid mixture. The mixture was stirred with methanol (80 mL), filtered to remove NaCl and the filtrate was evaporated to yield a sticky oil. This process was repeated again from the methanol stage giving 4.1 g (90%) of a colorless sticky oil **10**. ^{1}H NMR ($CDCl_3$): 6.8–6.9 (b, 5H, –Ph), 3.24 (s, 2H, CH_2Ph), 2.1–2.4 (m, 16H, $-CH_2NH-$), 0.7–1.4 (b, 6H,$-NH_2$); ^{13}C NMR: 139.5, 128.6, 128.6, 128.0, 126.7, 59.1, 54.0, 52.4, 47.2 41.6. Mass (m/z) = 206 (M–73), 134, 91.

4.2.5. 7-Benzyl-15-fluoro-1,4,7,10,13-pentaazacyclohexadecan-14,16-dione (5)

N7-benzyl pentaamine **10** (1.75 g, 6.27 mmol) and diethyl fluoromalonate (1.10 g, 6.18 mmol) were heated to reflux in anhydrous ethanol (300 mL) for 24 h. Evaporation of the solvent and recrystallization from methanol–acetonitrile gave 0.53 g (24%) of a white solid **5**. ^{1}H NMR ($CDCl_3$): 7.1–7.4 (m, 7H,), 5.21 (d, $J = 47.7$ Hz, 1H, –CHF), 3.48 (m, 4H), 3.36 (m, 2H), 2.55 (b, 12H), 1.57 (b, 2H); ^{13}C NMR ($CDCl_3$): 165.4 (d, $J = 6.8$ Hz), 139.7, 128.8, 128.5,

127.0, 86.8 (d, $J = 65.3$ Hz), 59.3, 54.7, 48.7, 47.1, 39.7; IR (KBr): 1688 (C=O), 1506, 1452 cm^{-1}; FAB-MS (m/z) = 366 (M + 1); Anal. Calcd for $C_{18}H_{29}N_5O_2F$: C, 59.00; H, 7.98; N, 19.11. Found: C, 59.24; H, 7.73; N, 19.15.

4.2.6. N-(2-Aminoethyl)-2 aminoacetylamide (11)

Glycine methyl ester hydrochloride (8 g, 0.0637 mol) was added in batches to a neat ethylenediamine solution over 1 h at 90°C with continuous stirring. After complete addition, the reaction mixture was heated to 120°C for an additional 6 h. Excess ethylenediamine was removed by distillation under reduced pressure. The residue was treated with 4 M aqueous NaOH (25 mL) with stirring for 30 min. The solvent was evaporated, and the residue was extracted with methanol, repeating this process as mentioned for **10**, and giving 7.4 g (95%) of a pale brown sticky oil, **11**. ^{1}H NMR (D_2O): 3.2–3.4 (m, 4H, $-NCH_2CO-$, $CONCH_2$), 2.74 (m, 2H, $-CH_2NH_2$); ^{13}C NMR (D_2O): 175.6, 43.9, 41.5, 39.8.

4.2.7. N,N'-Bis-(N-carbobenzyloxy-L-phenylalanyl)-triazaheptan-3-one (12)

A solution of diaminoamide **11** (2.08 g, 0.0176 mol) in methanol (120 mL) was added to a DMF (50 mL) solution of N-carbobenzyloxy-L-phenylalanyl-N-hydroxysucciniimide ester (14 g, 0.0353 mol) at room temperature. The solution gradually turned to a cloudy suspension and was allowed to stir for an additional 18 h. The mixture was filtered to collect the solid which was washed with methanol several times to provide 9 g (75%) of a pure white solid, **12**: ^{1}H NMR (DMSO-d_6): 8.33 (b, 1H), 8.12 (b, 1H), 7.81 (1H), 7.60 (D, 1H, $J = 8.4$ Hz), 7.51 (1H, J = 8.4 Hz), 7.1–7.4 (m, 20H), 4.93 (s, 4H, $-OCH_2Ph$), 4.27 (m, 1H), 4.17 (m, 1H), 3.69 (b, 2H), 2.9–3.3 (m, 6H), 2.74 (dd, 2H); ^{13}C NMR (DMSO-d_6): 174.1, 172.3, 172.1, 169.3, 156.5, 156.3, 138.6, 137.5, 137.4, 129.7, 128.8, 128.5, 128.2, 127.9, 126.7, 71.6, 65.8, 65.7, 58.6, 58.5, 56.8, 56.7, 42.7, 25.6.

4.2.8. N,N'-Bis-(L-phenylalanyl)-triazaheptan-3-one (13)

A solution of the di-N-Cbz compound **12** (9 g, 0.0132 mol) and 10% Pd on activated carbon (0.5 g) suspended in methanol (150 mL) was treated with H_2 (55 psi) at 50°C for 12 h. The solution was filtered through Celite, and the filtrate was evaporated to produce 5.44 g (100%) of a colorless sticky oil, **13**. ^{1}H NMR ($CDCl_3$): 8.19 (b, 1H), 7.92 (b, 1H), 7.66 (b, 1H), 7.1–7.3 (m, 10H), 3.2–3.9 (m, 12H), 2.4–2.8 (m, 4H); ^{13}C NMR ($CDCl_3$): 176.4, 175.1, 174.8, 170.0, 137.7, 137.5, 129.3, 128.0, 126.9, 56.5, 56.3, 42.9, 40.7, 40.2, 38.8.

4.2.9. 2S,12S-Dibenzyl-1,4,7,10,13-pentaazatridecane (14)

Triamide **13** (3.3g, 0.0108 mol) was allowed to react with 1.0 M BH_3–THF (250 mL) as previously described for **10** to provide a hydrochloride salt **14** · 10HCl. ^{1}H NMR (D_2O): 7.2–7.5 (m, 10H, –Ph), 3.97 (m, 2H), 3.4–3.6 (m, 12H), 3.22 (d, $J = 6.3$ Hz, 1H), 3.17 (d, $J = 6.3$ Hz, 1H), 3.02 (d, $J = 8.4$ Hz, 1H), 2.98 (d, $J = 8.7$ Hz, 1H); ^{13}C NMR (D_2O): 134.2, 129.6, 128.8, 50.1, 49.3, 44.0, 44.65, 44.50, 36.5. Anal. Calcd. for $C_{22}H_{35}N5 \cdot 9HCl$: C, 37.87; H, 6.36; N, 10.04. Found: C, 37.33; H, 6.06, N, 9.79.

To obtain the free base, the previous procedure was followed producing 2.69 g (93% overall yield) of **14** as a colorless oil. ^{1}H NMR ($CDCl_3$): 7.14–7.30 (m, 12H), 3.05 (m, 2H), 2.60–2.80 (m, 12), 2.46 (dd, $J = 19.5$ Hz, 8.7 Hz, 4H), 1.292 (b, 3H, –NH); ^{13}C NMR ($CDCl_3$): 139.3, 129.3, 128.5, 126.2, 56.3, 52.7, 49.7, 49.5, 42.9.

4.2.10. 2S,12S-Dibenzyl-15-fluoro-1,4,7,10,13-pentaazacyclohexadecan-14,16-dione (6)

Dibenzylpentaamine **14** (1.38 g, 3.74 mmol) and diethyl fluoromalonate (0.94 g, 5.2 mmol) were heated to reflux in anhydrous ethanol for one week. The solution turned yellow. Evaporation of the solvent and recrystallization from acetonitrile provided 350 mg (21%) of **6** as white needles. ^{1}H NMR ($CDCl_3$): 7.1–7.3 (m,

11H), 6.77 (t, 1H, CONH–), 5.02 (d, $J = 47.4$ Hz, 1H), 4.3–4.5 (m, 2H), 2.5–2.9 (m, 16H), 1.37 (b, 3H); ^{13}C NMR ($CDCl_3$): 166.6 (d, $J = 6.5$ Hz), 163.0 (d, 6.8 Hz), 137.4 (d, $J =$ 17.7 Hz), 137.7, 137.0, 129.1, 129.2, 128.6, 128.5, 126.8, 126.6, 53.6, 52.2, 50.4, 50.3, 49.3, 49.0, 48.7, 48.3, 39.7, 39.3. IR (KBr): 1678, 1668 (C=O), 1534, 1451 cm^{-1}; FAB-MS (m/z) = 455 (M + 1); Anal. Calcd. for $C_{25}H_{34}N_5O_2F$: C, 65.91; H, 7.52; N, 15.37. Found: C, 65.75; H, 7.59; N, 15.31.

4.3. Nickel complexes

4.3.1. 7-Benzyl-15-fluoro-1,4,7,10,13-pentaazacyclohexadecane-14,16-dione nickel(II) acetate complexes (5 · Ni)

Macrocycle **5** (67 mg, 0.184 mmol) dissolved in methanol (3 mL) was added to a methanol solution of nickel(II) acetate (45 mg, 0.181 mmol). The color of the solution changed to purple. After evaporation of the solvent, a gray powder was obtained in 54 mg (90%) of **5 · Ni**. FAB-MS (m/z) = 421 (M + 1); UV/vis: λ_{max} (in water) 350 ($\epsilon = 37$ cm^{-1} M^{-1}), 498 $\epsilon = 29$ cm^{-1} M^{-1}) nm; IR (KBr): 1616 (C=O),1576, 1450 cm^{-1}. After exposure to air for 24 h, the color of the nickel complex changed from purple to orange. Evaporation of the solvent gave an orange powder with UV/vis λ_{max} (H_2O) 310 ($\epsilon = 1040$ cm^{-1} M^{-1}), 486 ($\epsilon = 56$ cm^{-1} M^{-1}) nm; FAB-MS (m/z) = 328 (M—Ph).

4.3.2. 2S,12S-Dibenzyl-15-fluoro-1,4,7,10,13-pentaazacyclohexadecan-14,16-dione nickel(II) complex (6 · Ni)

The procedure was similar to that described above. A green nickel(II) complex was produced in methanol from ligand **6** and $Ni(OAc)_2$ without base treatment. UV/vis: $\lambda_{max} = 372$ nm; FAB-MS (m/z) = 512 (M + 1), IR (KBr): 1700 (C=O), 1560 cm^{-1}. After treating with 2.1 eq. NaOH, purple crystals of **6 · Ni** were obtained from crystallization in methanol–water solution in 96% yield. Unfortunately, the complex formed was no longer soluble in solvents such as methanol, ethanol, water, $CHCl_3$, DMF, and benzene. UV/vis (CH_3OH): $\lambda_{max} = 358$ and 508 nm (ϵ not determined due to insolubility); IR (KBr): 1600 (C=O), 1572, 1456 cm^{-1}. FAB-MS (m/z) = 512 (M + 1). Anal. Calcd. for $NiC_{25}H_{32}N_5O_2F \cdot (1/2)H_2O$: C, 57.61; H, 6.29; N, 13.45. Found: C, 57.86; H, 6.30; N, 13.41.

Acknowledgements

The authors thank the National Science Foundation (grant no. CHE-9521216 to C.J.B.) and the American Cancer Society (grant no. CN-72 to S.E.R.) for support of this work.

References

[1] F.P. Bossu, E.B. Paniago, D.W. Margerum, S.T. Kirksey, Jr. and J.L. Kurtz, Inorg. Chem. 17 (1978) 1034.
[2] A. Böttcher, H. Elias, L. Müller and H. Paulus, Angew. Chem. Int. Ed. Engl. 31 (1992) 623.
[3] A. Berkessel, J.W. Bats and C. Schwarz, Angew. Chem. Int. Ed. Engl. 29 (1990) 106.
[4] C. Bolm, G. Schlingloff and K. Weickhardt, Tetrahedron Lett. 34 (1993) 3405.
[5] R. Irie, Y. Ito and T. Katsuki, Tetrahedron Lett., 32 (1991) 6891.
[6] T. Yamada, T. Takai, O. Rhode and T. Mukaiyama, Bull. Chem. Soc. Jpn. 64 (1991) 2109.
[7] W. Nam, H.J. Kim, S.H. Kim, R.Y.N. Ho and J.S. Valentine, Inorg. Chem. 35 (1996) 1045.
[8] E. Kimura, R. Machida and M. Kodama, J. Am. Chem. Soc. 106 (1984) 5497.
[9] E. Kimura, A. Sakonaka, R. Machida and M. Kodama, J. Am. Chem. Soc. 104 (1982) 4255.
[10] C.-C. Cheng, S.E. Rokita and C.J. Burrows, Angew. Chem. Int. Ed. Engl. 32 (1993) 277.
[11] D. Chen, R.J. Motekaitis and A.E. Martell, Inorg. Chem., 30 (1991) 1396.
[12] C.J. Burrows and S.E. Rokita, Acc. Chem. Res. 27 (1994) 295.
[13] E. Kimura, M. Shionoya, M. Okamoto and H. Nada, J. Am. Chem. Soc. 110 (1988) 3679.
[14] C.-C. Cheng, Ph.D. thesis, State University of New York at Stony Brook, 1993.
[15] R. Machida, E. Kimura and Y. Kushi, Inorg. Chem. 25 (1986) 3461.

[16] E. Kimura, H. Anan, T. Koike and M. Shiro, J. Org. Chem. 54 (1989) 3998.
[17] B. Newmann, S.C. Müller, M.J.B. Hauser, O. Steinbock, R.H. Simoyi and N.S. Dalal, J. Am. Chem. Soc. 117 (1995) 6372.
[18] K.S. Kasprzak, Chem. Res. Toxicol. 4 (1991) 604.
[19] D.F. Smith, in: International Critical Tables of Numerical Data for Physics, Chemistry and Technology, ed. E.W. Washburn, Vol. 3 (McGraw-Hill, New York) p. 271.